

Central Lancashire Online Knowledge (CLoK)

Title	Identification of the multifaceted chemopreventive activity of curcumin against the carcinogenic potential of the food additive, KBrO ₃
Type	Article
URL	https://clock.uclan.ac.uk/21264/
DOI	https://doi.org/10.2174/1381612824666171226143201
Date	2017
Citation	Obaidi, Ismael, Higgins, Michael, Bahar, Bojlul, Davis, Jessica L. and McMorrow, Tara (2017) Identification of the multifaceted chemopreventive activity of curcumin against the carcinogenic potential of the food additive, KBrO ₃ . <i>Current Pharmaceutical Design</i> , 24 (5). pp. 595-614. ISSN 1381-6128
Creators	Obaidi, Ismael, Higgins, Michael, Bahar, Bojlul, Davis, Jessica L. and McMorrow, Tara

It is advisable to refer to the publisher's version if you intend to cite from the work.
<https://doi.org/10.2174/1381612824666171226143201>

For information about Research at UCLan please go to <http://www.uclan.ac.uk/research/>

All outputs in CLoK are protected by Intellectual Property Rights law, including Copyright law. Copyright, IPR and Moral Rights for the works on this site are retained by the individual authors and/or other copyright owners. Terms and conditions for use of this material are defined in the <http://clock.uclan.ac.uk/policies/>

Identification of the multifaceted chemopreventive activity of curcumin against the carcinogenic potential of the food additive, KBrO₃

Ismael Obaidi¹, Michael Higgins¹, Bojlul Bahar², Jessica L. Davis¹, and Tara McMorrow¹

¹ UCD Centre for Toxicology, School of Biomedical and Biomolecular Sciences, Conway institute, University College Dublin, Ireland.

² International Institute of Nutritional Sciences and Applied Food Safety Studies, University of Central Lancashire, Preston, PR1 2HE, United Kingdom

* Correspondence: Ismael.obaidi@ucdconnect.ie



Abstract:

Background: Potassium bromate (KBrO₃), a food additive, has been used in many bakery products as an oxidizing agent. It has been shown to induce renal cancer in many *in-vitro* and *in-vivo* experimental models

Objectives: This study evaluated the carcinogenic potential of potassium bromate (KBrO₃) and the chemopreventive mechanisms of the anti-oxidant and anti-inflammatory phytochemical, curcumin against KBrO₃-induced carcinogenicity

Method: Lactate dehydrogenase (LDH) cytotoxicity assay and morphological characteristics were used to assess curcumin's cytoprotective potential against KBrO₃ toxicity. To assess the chemopreventive potential of curcumin against KBrO₃-induced oxidative insult, intracellular H₂O₂ and the nuclear concentration of the DNA adduct 8-OHdG were measured. PCR array, qRT-PCR, and western blot analysis were used to identify dysregulated genes by KBrO₃ exposure. Furthermore, immunofluorescence was used to evaluate the ciliary loss and the disturbance of cellular tight junction induced by KBrO₃.

Results: Oxidative stress assays showed that KBrO₃ increased the levels of intracellular H₂O₂ and the DNA adduct 8-OHdG. Combination of curcumin with KBrO₃ efficiently reduced the level of H₂O₂ and 8-OHdG while up-regulating the expression of catalase. PCR array, qRT-PCR, and western blot analysis revealed that KBrO₃ dysregulated multiple genes involved in inflammation, proliferation, and apoptosis, namely CTGF, IL-1, and TRAF3. Moreover, qRT-PCR and immunofluorescence studies showed that KBrO₃ negatively affected the tight junctional protein (ZO-1) and induced a degeneration of primary ciliary proteins. The negative impact of KBrO₃ on cilia was markedly repressed by curcumin.

Conclusion: Curcumin could potentially be used as a protective agent against carcinogenicity of KBrO₃

Keywords:

Potassium bromate (KBrO₃); chemoprevention; curcumin; primary cilia; kidney cancer; inflammation

1. INTRODUCTION

Potassium bromate (KBrO₃), a food additive, has been used in different bakery products as an oxidizing agent. In 2005, the use of KBrO₃ as a food additive was banned by countries of the European Union, Canada, Japan, China, India, and South America. Surprisingly, it has not been banned by the FDA in the US and still can be found in some bakery products [1, 2]. KBrO₃ was shown to induce renal cancer in many *in-vitro* and *in-vivo* experimental models [3-5]. Shiao *et al* found that rats exposed to KBrO₃ in drinking water caused a mutation in the Von Hippel-Lindau tumor (VHL) gene, a crucial tumor suppressor that has been found to be

mutated in renal cell carcinomas [6]. KBrO_3 , was found to induce oxidative DNA damage and DNA adduct formation that lead to various gene mutations. For instance, the formation of the mutagenic 8-hydroxy deoxyguanosine (8-OHdG) was detected following the exposure of porcine kidney cells to KBrO_3 [7]. Interestingly, KBrO_3 was found to interact with GSH to form the highly reactive 8-oxodeoxyguanosine (8-oxodG), thus causing DNA double strand break [8, 9] .

Following DNA damage, many genes including those controlling apoptosis and inflammation are dysregulated. For instance, Bader and Hsu mentioned that many pro-inflammatory genes such as HIF1a, HIF2a, TNF- α , TGF- β , and NF-KB were found to be up-regulated in response to DNA damage that eventually induced VHL mutation [10] .

Primary cilia are immotile sensory organelles that play an important role in cell differentiation, polarity, and quiescence. They can receive mechanical and chemical signals from other cells as well as, from the surrounding environment [11]. Normally, cells assemble cilia on their membranes when they "stop" dividing, exit the cell cycle, and start to differentiate [12]. However, cells tend to lose cilia when they re-enter the cell cycle and mitosis [13]. In most renal cell carcinomas where the suppressor VHL gene is inactivated, Schraml *et al* found that ciliary loss in clear cell renal cell carcinoma (ccRCC) was strongly associated with the mutation of this tumor suppression gene. In contrast, the author found that in papillary renal cell carcinomas, the frequency of cilia was higher than ccRCC and the ciliary loss was VHL independent, which points to the differences in the biological pattern between these types of cancer cells [14].

Chemoprevention is a novel aspect in cancer development and treatment referring to the use of natural, semi-synthetic or synthetic compounds to halt, stop, or reverse tumor formation and progression [15]. Chemopreventives can block tumor initiation; therefore, they are termed blocking agents. For instance, anti-oxidants, free radical scavengers, phase I drug-metabolizing enzymes inhibitors, and phase II drug-metabolizing enzymes inducers are deemed cancer blocking agents. Whereas compounds that halt the stages of tumor promotion and progression are referred to as tumor suppressors. Induction of apoptosis, terminal cell differentiation, inhibition of cell proliferation and clonal expansion, and alteration of gene expression of preneoplastic tumors are examples of tumor suppression [15-17] .

Curcumin, also known as diferuloylmethane, is a polyphenolic compound derived from the root and rhizome of the plant *Curcuma longa* [18, 19]. Curcumin has a chemoprevention potential owing to its anti-oxidant, anti-inflammatory, immunomodulatory, and pro-apoptotic potential[20]. While curcumin abrogates several oncogenic pathways such as NF-KB, Akt/PI3K and MAPK, it has recently been found to induce anti-tumor potential via epigenetic modulations of critical genes. For instance, it dysregulates several oncogenic and tumor suppressor miRNA, namely, miR-21, miR-17-5p, miR-22, miR-15a, miR-20a, and miR-27a [21, 22]

This study aimed at investigating the carcinogenic potential of KBrO_3 and the mechanisms by which curcumin can prevent the carcinogenic insults of KBrO_3 on the renal epithelial cells (RPTEC/TERT1). Moreover, our group has reported that targeting RPTEC/TERT1 with a subtoxic concentration of KBrO_3 was associated with loss of primary cilia [23], therefore this study also investigated the preventive potential of curcumin against KBrO_3 induced deciliation, and thus inhibited proliferation and dedifferentiation.

2. MATERIALS AND METHOD

2.1. Cell culture and treatment

The human renal proximal tubular epithelial (RPTEC/TERT1) [24] and ACHN cell lines were obtained from the American Tissue Culture Collection (ATCC). Cells were maintained in low glucose (5 mM) Dulbecco's Modified Eagle / Nutrient Mix F-12 medium supplemented with 5 µg/ml insulin, 5 µg/ml transferrin, 5 µg/ml selenite (ITS), 36 ng/ml hydrocortisone, 10 ng/ml epidermal growth factor (EGF) (Sigma-Aldrich) 50 U/ml penicillin, 50 µg/ml streptomycin (P/S), and 2 mM L-glutamine (Gibco, Life Technologies). ACHN cells were maintained in Minimum Eagle Medium (Sigma-Aldrich) with 10% FBS and P/S. Both cell lines were incubated at 37° C in a 5% CO₂ humidified atmosphere.

RPTEC/TERT1 were seeded at a density of 1x10⁶ cells/ml. Cells were maintained for 10 days after reaching 100% confluency to allow stabilization of the monolayer [23]. While ACHN cells were seeded at the same density one day in advance before the treatment. KBrO₃ and curcumin were purchased from (Sigma-Aldrich, Taufkirchen, Germany). KBrO₃ was dissolved in water to prepare 100mM stock solution which was then further diluted with culture medium to get the indicated concentrations. Curcumin and silymarin were dissolved in DMSO to prepare stock solutions of 250 mM and 50mM, respectively. They were then further diluted with culture medium to final concentration 200 µM and 25 µM, respectively. In most experiments, where curcumin or silymarin was used, control cells were exposed to a maximum 0.1% DMSO.

2.2. Lactate dehydrogenase(LDH) release assay (LDH)

The LDH assay was performed using a Roche kit (Roche Diagnostics, Mannheim, Germany). Briefly, RPTEC/TERT1 cells were cultured at density of 1x10⁶ cells/ ml in 24-well plates and allowed to form a fully confluent monolayer. 10 days post confluency, cells were treated with six different concentrations of KBrO₃ (0.5,1,2,3,5, and 10 mM) only or in a combination with 25µM curcumin for 24h. The positive control for maximum LDH release or 100% cell death was prepared by treating cells with 2% Triton-X 100 for 5 min at 37°C. Following 15min incubation of cell supernatants with the reaction mixture (provided by the kit), the absorbance was measured at 490nm using Spectamax2 plate reader (Molecular devices, Winnersh/ UK). LDH release was expressed as a percentage of the maximum LDH activity.

2.3. Phase contrast microscopy

RPTEC/TERT1 cells at 1x10⁶ cells/ ml were cultured in 24- well plates and allowed to form a fully confluent monolayer. 10 days post-confluency, cells were treated with KBrO₃ (10mM) only or in a combination with 25µM curcumin for 24h at 37°C. Cellular morphology was observed by phase contrast microscopy using a JVC high-resolution digital camera (KY-F55BE) attached to a Nikon TMS phase contrast microscope. Micrographs were processed using ImageJ v.1.49.

2.4. Determination of intracellular H₂O₂ concentration

Intracellular hydrogen peroxide (H₂O₂) concentrations were measured using Amplex red assay kit (Thermo Fisher scientific, Carlsbad, CA) following the manufacturer instructions. Briefly, cells were cultured in 12 well culture plates. Following treatment, cells were lysed in 200 µl ice-cold lysis buffer (0.1% Triton X-100 in 0.05 M sodium phosphate buffer, pH 7.4). Following this, lysates were transferred to pre-chilled microfuge tubes and vortexed every 3 min for 15 min for complete cell homogenization. Tubes were centrifuged at 14,000 g at 4°C for 15 min. A volume of 50 µl of supernatants and standard H₂O₂ solutions (0, 0.05, 0.1,

0.25, 0.5, 0.75, 1, 1.25, 2, and 5 μM) were loaded in 96-well opaque black microplate. An equal volume of Amplex Red reaction mixture (0.1 mM Amplex red reagent and 0.2 U/ml horseradish peroxidase in 1X reaction buffer) was added to the pre-loaded wells to initiate the reaction. The fluorescence was measured kinetically every 30 sec for 30 min at excitation and emission wavelengths of 530 and 590 nm, respectively using a scanning microplate reader (Molecular Devices Inc, Sunnyvale, CA, USA). Intracellular H_2O_2 concentration was calculated using the standard curve and normalized to the total protein content.

2.5. Determination of intra-nuclear concentration of 8-OHdG

This assay consists of 4 stages: DNA extraction, determination of DNA concentration, DNA digestion, and measuring the concentration of the DNA adduct 8-OHdG.

DNA was extracted from cells using WAKO DNA Extractor WB Kit (Wako, Osaka, Japan) which contains sodium iodide (NaI) as chaotropic agent to minimize the oxidation of DNA during the extraction. The concentrations of DNA solutions were calculated using the Thermo Fisher Scientific NanoDrop 2000 (Thermo Fisher Scientific, Wilmington, DE, USA). The Wako 8-OHdG Assay Preparation Reagent kit was used exclusively to digest DNA and release 8-OHdG. Determination of the intranuclear 8-OHdG concentration was performed using an enzyme-linked immunosorbent assay (ELISA) kit (Highly Sensitive 8-OHdG Check ELISA kit, Japan Institute for the Control of Aging, Fukuroi, Japan). Briefly, a volume of 50 μl of digested DNA samples and standard concentrations were loaded to the provided ELISA plate. A volume of 50 μl primary antibody per a well was added and incubated overnight at 4°C. Next day, the well contents were poured off and washed three times using 250 μl /well washing solution. The wells were incubated with 100 μl / well of secondary antibody for 1h at room temperature. The plate was washed before adding a chromatic solution and incubated for 15 min at room temperature in a dark place. Finally, the reaction was terminated by adding 100 μl of the reaction terminating solution. The absorbance was read at 450 nm.

2.6. Immunofluorescent labeling

For immunofluorescent labeling experiments, cells were cultured in 8-well chamber slides (Millipore, USA) and allowed to form a fully confluent monolayer. 10 days post-confluency, cells were treated with DMSO-containing medium, 5.5mM KBrO_3 , 25 μM curcumin, or a combination of both for 24h at 37 °C. Following treatment, cells were washed with PBS three times and fixed with 3.7% formaldehyde for 20 min at room temperature. Cells were then washed three times with PBS and permeabilized with 0.2% (v/v) Triton-X 100 in PBS. Background was reduced by blocking nonspecific signals with 0.5% (w/v) BSA in PBS. The ciliary markers Acetylated α -tubulin and Arl 13B were labeled using a mouse anti-human antibody (1:400) (Sigma-Aldrich, Taufkirchen, Germany) and a rabbit anti-human antibody, respectively. ZO-1 was labeled using a rabbit anti-human antibody (1:300) (Zymed, Invitrogen, South San Francisco, CA). Nuclei were stained with Hoechst 33342 (1:1000) (Sigma-Aldrich, Taufkirchen, Germany). Slides were imaged using a Zeiss A-Plan 40X/0.65 objective and a Zeiss M1 Upright AxioImager with CoolLED P3000 light source or a Zeiss C-Plan-Apochromat 40X/1.3 objective and a Zeiss LSM510 UVMETA confocal microscope. Images were deconvolved using Auto Quant-X3 deconvolution software (Version 3.0.3) (Media Cybernetics Inc.) at 5 iterations. Images were adjusted for brightness and contrast using Fiji/ImageJ (Fiji.sc/).

2.7. RNA extraction and preparation of cDNA

RPTEC/TERT1 cells were seeded and treated as described earlier using 6-well plate format. TRIzol method was used to extract total RNA. The same method was applied to extract the total RNA from the ACHN cells after 24h of growth. Briefly, TRIzol (Life Technologies, USA) was used to lyse cells (1ml per a well). Cells were then homogenized by passing through pipette tip several times. Following the homogenization, 200 μ l of 1-bromo-3-chloropropane (BCP), a chloroform derivative, was added to the homogenate, mixed by vortexing, incubated for 3 min at room temperature, then centrifuged at 12,000 \times g at 4°C for 15min. The mixture was separated into three phases: aqueous (RNA), interphase and a red lower organic layer (DNA and protein). The aqueous phase was transferred into a clean microfuge tubes then 500 μ l isopropanol was added to precipitate RNA. Following centrifugation at 12,000 \times g at 4°C for 15 min, the supernatant was discarded and the pellets were washed with 500 μ l of 75% ethanol to remove further impurities. The microfuge tubes were finally centrifuged at 7500g at 4°C for 5 min. The supernatant was discarded and RNA pellets were dissolved in ddH₂O. For further RNA purification and removing of genomic DNA contamination, mRNeasy and DNase Max kit (Qiagen, UK) were used according to the manufacturer protocol. The yield of the RNA was assessed by measuring the optical density at 260 nm and 280nm using a Nanodrop ND-1000 spectrophotometer (Thermo Fisher Scientific, Wilmington, DE, USA). The purity of RNA samples was assessed based on the absorbance ratio of 260:280 which should be \geq 1.8. A total RNA of 1 μ g was reversed transcribed to cDNA using a RevertAid H Minus First Strand cDNA synthesis Kit (Fermentas GmbH, St. Leon-Rot, Germany) according to the manufacturer's instructions.

2.8. Quantitative Real-Time PCR Analysis

Quantitative expression of a total of 192 genes (list of genes provided in the supplementary Table1) involved in inflammation, angiogenesis, and apoptosis were evaluated using real-time PCR ABI PRISM® 7900HT (Foster City, California USA). These were customized PCR arrays designed by (Sigma-Aldrich, Taufkirchen, Germany) Corp. For the PCR array experiment, 20 μ L cDNA of each individual treatment was diluted up to 170 μ L using distilled water. Three biological replicates of a single treatment group were pooled and analyzed. The real-time PCR mix (20 μ L/well) contained 1 μ L of pooled cDNA, 3 μ L water, 6 μ L primer mix, and 10 μ L SYBR green master mix. The thermal cycle conditions were 95°C for 15min followed by 45 cycles of 94°C for 15 sec, 55 °C for 30 sec, and 70 °C for 30 sec. The dissociation stage was set at 95 °C for 15 sec, 60°C for 15 sec, and 95°C for 15 sec, as previously described [25] The mRNA abundances were expressed in "cycle threshold" (Ct) values, which represents the number of PCR cycles after which the PCR product crosses a threshold value. A Ct value of 35 was used as the cut-off limit. The normalization of gene expression was carried out based on the abundance of the house-keeping genes β actin (*ACTB*), glyceraldehyde 3-phosphate dehydrogenase (*GAPDH*) and beta-glucuronidase (*GUSB*).

Validation of the PCR array was performed using single tube TaqMan-probe based gene expression assays (Applied Biosystems, Foster City, CA, USA). Normalization of genes expression was carried out using the house-keeping gene β -actin. The PCR reaction mixture (10 μ L) consisted of 0.5 μ L cDNA, 3.5 μ L nuclease free water, 0.5 μ L primer mix, 0.5 μ L loading control (β -actin), and 5 μ L TaqMan master mix. The thermal cycle conditions were as follows: 50°C for 2 min, 95 °C for 10 min followed by 40 cycles of 95 °C for 15 s, 60 °C for 1 min. Samples were loaded in an optical 384 well plate in duplicates (10 μ L/ well) and Ct values <35 were used as the cut-off limit. For the analysis of both PCR array and qRT-PCR, the $2^{-\Delta\Delta Ct}$ method was applied. Briefly, average ΔCt was calculated as the difference of Ct values of any target gene from the average of the Ct

value of the reference gene (s). Then, fold change was calculated as $2^{(-\text{average } \Delta\text{Ct target gene})/2^{(-\text{average } \Delta\text{Ct reference gene})}}$. A fold difference cut-off point was set at ≥ 2.0

2.9. Western blot analysis

Western blot analysis was carried out according to the standard method by Buchmann [26]. Following cell treatment, the media was removed, and the cells were lysed by using RIPA buffer (Sigma-Aldrich, Taufkirchen, Germany). Total protein concentration was determined by Bradford method using BCA protein assay kit (Pierce, Rockford, IL, USA) according to the manufacturer protocol. Equal amounts of 20 μg of whole cell lysates were placed in each lane and subject to SDS-PAGE electrophoresis, then transferred to a 0.2 μm pore size Whatman Protran[®] nitrocellulose membrane (Thermo Fisher Scientific, Wilmington, DE, USA) using a semi-dry transfer system. After the transfer, the membranes were blocked by incubation with TBS-T buffer (50 mM tris-HCl, pH 7.4, 150 mM NaCl, and 0.05% Tween 20) containing 5% non-fat milk or BSA for 1hr at room temperature. The membranes were then incubated overnight at 4°C with CTGF primary antibody (1:1000) (Santa Cruz, USA) and GAPDH (1:10,000) (Cell Signaling Technology Inc, Danvers, MA, USA). Next day, the blots were washed with T-BST then incubated with TBS-T/ 5% non-fat milk containing an appropriate secondary antibodies coupled with horse radish peroxidase (HRP) (Cell Signaling Technology Inc, Danvers, MA, USA) for 1h at room temperature. Immunodetection was performed using the SuperSignal West Pico Substrate (Thermo Scientific, Rockford, IL, USA).

2.10. Statistical Analysis

All experiments were repeated at least three times. Statistical analyses were performed using Graph Pad Prism 5.0. Data was analyzed using one-way analysis of variance (ANOVA). Comparisons between different treatment groups were made by Newman-Keuls Multiple Comparison post-test. Results were expressed as the mean \pm standard error of the mean (SEM). A probability of 0.05 or less was deemed statistically significant.

3. Results

3.1. Curcumin protected RPTEC/TERT1 against KBrO₃-induced cytotoxicity

The potential cytoprotective effect of curcumin was investigated by comparing the activity of the released LDH following the exposure to KBrO₃ alone and KBrO₃/ curcumin combination. The morphological pattern of cells was assessed using phase contrast microscopy. As shown in *Fig. 1a*, KBrO₃ sharply increased the relative activity of LDH at 10mM KBrO₃ concentration. The combination of KBrO₃ with curcumin exhibited an extremely significant ($p < 0.001$) lowering of LDH release compared to KBrO₃ treatment only. These findings revealed that curcumin exhibited a cytoprotective potential against KBrO₃ induced cell death

The effect of each treatment on cellular morphology was assessed using phase contrast microscopy (*Fig. 1b*). When RPTEC/TERT1 cells were treated with DMSO (i) or with curcumin (ii), the cells showed normal cobblestone appearance, tight interconnections, and formed characteristic domes. Such morphological characteristics reflect an intact cellular transport system and indicated that the cells were “happy”, “healthy”, and fully differentiated. Under toxic conditions (iii), KBrO₃ caused severe cellular damage with a complete loss of domes and loss of tight junctions between cells. Curcumin clearly minimized KBrO₃-induced cellular damage

and loss of tight junctions. However, it only partially re-established the characteristic domes of RPTEC/TERT1 cells (Fig.1.b).

Following 24h exposure, the toxic (IC₅₀) and the subtoxic (IC₁₀) concentrations of KBrO₃ were estimated to be 5.5 and 7.5mM, respectively using an LDH release assay (Fig.1c).

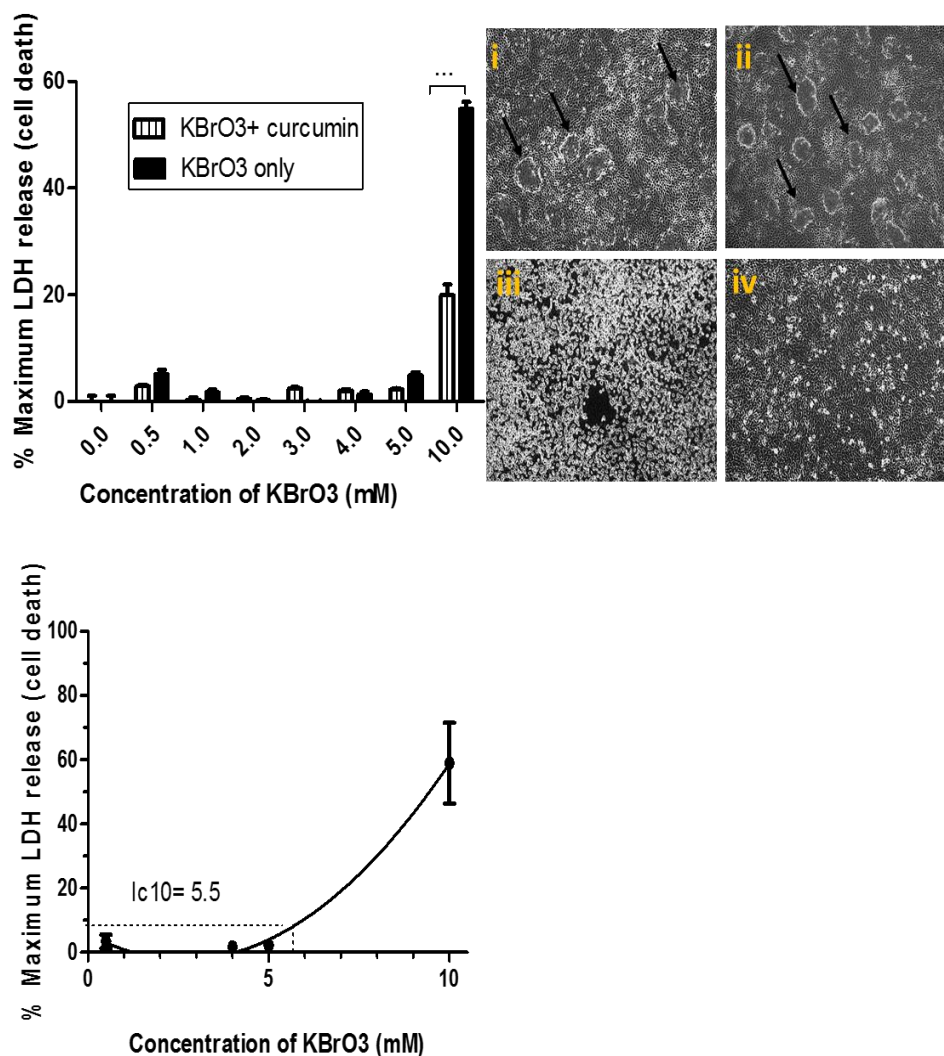


Figure 1. Examination of the cytoprotective effects of curcumin measured by cytotoxicity assay and assessed by morphological characteristics.

Fig.1a: The cytoprotective potential of curcumin was assessed using the LDH cytotoxicity assay. RPTEC/TERT1 cells were treated either with the indicated concentrations of KBrO₃ only or a combination of KBrO₃ concentrations with 25µM curcumin. The figure represents mean±SEM of six independent experiments. (***) = $p < 0.001$

Fig.1b: Analysis of the morphological characteristics of RPTEC/TERT1 cells. Cells were seeded in 24 well plates, 10 days post 100% confluency, the cells formed fluid filled domes which reflect a well-functioning transport system. (i) RPTEC/TERT1 were treated with 0.1% DMSO (control), or (ii) with 25µM curcumin for 24h. The domes were maintained and cells were morphologically unaffected by the treatment. (iii) Cells were treated with 10mM KBrO₃; (iv) Cells were treated with the combination of 10mM KBrO₃+ 25µM curcumin for 24 hr.

Fig.1c: Estimation of subtoxic IC10 and the toxic IC50 concentrations of KBrO3. RPTEC/TERT1 cells were seeded in 24 well plates. 10 days post 100% confluency, they were treated with the indicated concentrations of KBrO₃ to estimate subtoxic IC10 and the toxic IC50 concentrations. 2% Triton-TX100 was used as a positive control of cell death. The figure represents mean ± SEM of six independent experiments.

3.2. Curcumin suppressed KBrO₃ induced oxidative stress and DNA damage

The potential chemopreventive activity of curcumin was further assessed by comparing the level of oxidative stress following the exposure of RPTEC/TERT1 cells to KBrO₃ alone or in combination with curcumin. In this context, intracellular H₂O₂ and 8-OHdG concentrations were measured. Of note, at both IC10 and IC50 concentrations, KBrO₃ significantly increased the level of H₂O₂ ($p < 0.05$) (Fig.2a,b), and 8-OHdG ($p < 0.001$) (Fig.2c,d) compared to the control or curcumin-only treatment. The combination of curcumin with IC10 or IC50 KBrO₃ concentrations significantly ($p < 0.05$) inhibited the levels of both H₂O₂ and 8-OHdG compared to KBrO₃ treatment only (Fig.2a, b, c and d). In addition, KBrO₃ significantly ($p < 0.05$) reduced catalase gene expression compared to the control or curcumin only treatment. The combination of curcumin with KBrO₃, significantly ($p < 0.05$) reversed the negative effect of KBrO₃ by upregulating catalase gene expression (Fig.2e).

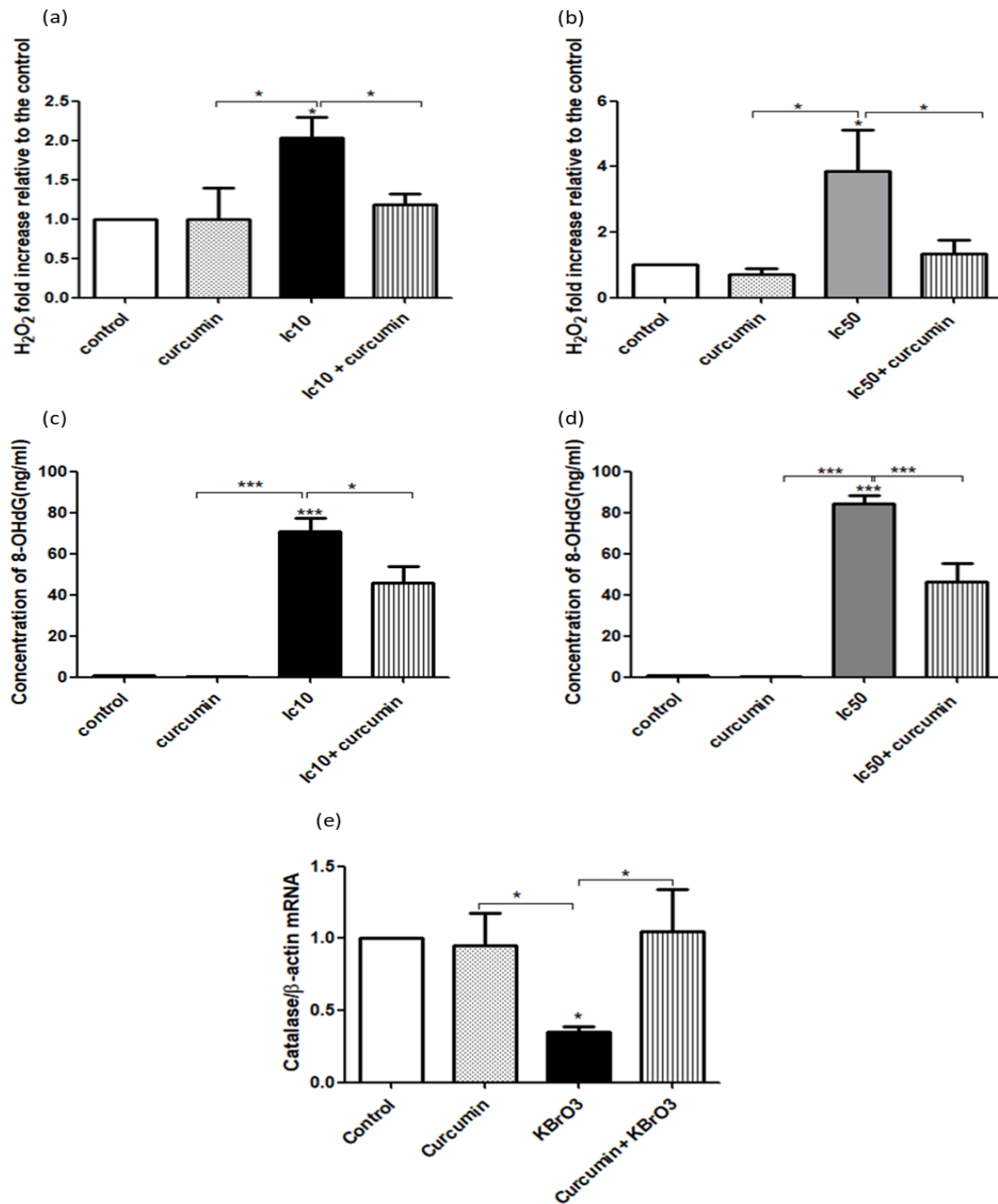


Figure 2. Analysis of Curcumin protection on RPTEC/TERT1 against KBrO₃ induced oxidative stress and DNA adduct formation

Fig.2a, b) Cells were seeded in 24 well plates until fully confluent. After 10 days, cells were treated with 0.1% DMSO (control), curcumin, KBrO₃ and a combination of KBrO₃ + curcumin. Intracellular concentration of H₂O₂ was detected using the *Amplex Red* Hydrogen Peroxide Assay Kit. The data represents three independent experiments, * = $p < 0.05$.

Fig.2c,d) DNA adduct formation was investigated by measuring the intracellular concentration of the DNA adduct 8-OHdG, using the Highly Sensitive 8-OHdG Check ELISA kit following the manufacturer kit instructions. The data represents three independent experiments. * = $p < 0.05$, ** = $p < 0.01$, and *** = $p < 0.001$.

Fig.2e) Catalase gene expression was examined in KBrO₃ (5.5mM) treated RPTEC/TERT1 cells after 24h treatment by RT-PCR analysis. (* = $P < 0.05$).

3.3. KBrO₃ induced dysregulation of target genes

The effects of KBrO₃ on a panel of 192 genes, was assessed using SYBR green based PCR array technology. These genes are involved in the regulation of inflammation, oxidative stress, angiogenesis, epithelial-mesenchymal transition (EMT), ciliary formation, and apoptosis (supplementary table 1).

Following the exposure of RPTEC/TERT1 cells to 5.5mM KBrO₃, many genes were dysregulated, as shown in table 1. Namely, connective tissue growth factor (CTGF) was the first most overexpressed gene, while interleukin (IL)1-receptor 1 (IL-1R1) was the first most downregulated compared to the untreated RPTEC/TERT1 cells. Genes that were differentially dysregulated in renal cancerous ACHN cells compared to normal RPTEC/TERT1 cells are shown in table 2. In this regard, CTGF was one of the top three most overexpressed genes, while IL-1R1 was the most down-regulated gene. The status of genes, that were up-/down-regulated following the exposure of RPTEC/TERT1 cells to KBrO₃, was compared to the congruent genes in ACHN cells. ACHN cell line was used as a positive control of carcinogenesis.

Interestingly, we found that a total of 47 genes were differentially dysregulated in the same manner in both KBrO₃ treated RPTEC/TERT1 and in the cancerous ACHN cell lines (Table 3).

Table 1: List of genes dysregulated following the exposure of RPTEC/TERT1 to KBrO₃ for 24h compared with untreated RPTEC/TERT1 cells

Genes with markedly increased expression			Genes with markedly decreased expression		
Gene	Gene name	Fold increase	Gene	Gene name	Fold decrease
CTGF	Connective tissue growth factor	197.55	IL1R1	Interleukin (IL)1-receptor 1	-57.7
PAI1	Plasminogen activator inhibitor-1	37.53	TLR3	Toll-like receptor 3	-30.89
RETN	Resistin	29.92	CXCL1	Chemokine (C-X-C Motif) Ligand 1	-26.57
FOS	Proto-oncogene c-Fos	28.21	IL8	Interleukin 8	-25
PIM3	Pim-3 Proto-Oncogene, Serine/Threonine Kinase	15.40	CXCL2	Chemokine (C-X-C Motif) Ligand 2	-23.08
SOCS1	Suppressor of cytokine signaling 1	16.24	TRAF5	TNF receptor-associated factor 5	-22.29
TNFA	Tumor necrosis factor	11.66	STAT1	Signal Transducer and Activator of Transcription 1	-20.26
TLR4	Toll-like receptor 4	11.28	TRAF3	TNF receptor-associated factor 3	-17.5
EGF	Epidermal growth factor	9.76	MYD88	Myeloid differentiation primary response	-17.49
LTA	Lymphotoxin-alpha	9.13	TRAF6	TNF receptor-associated factor 6	-13.3
NR4A2	Nuclear receptor related 1 protein	8.50	CCL20	Chemokine (C-C motif) ligand 20	-12.9
UBC	Ubiquitin C	7.02	IL6	Interleukin 6	-11.75
ADRB2	Adrenoceptor Beta 2, Surface	6.18	CASP1	Caspase 1, Apoptosis-Related Cysteine Peptidase	-11.59
IL2RA	Interleukin-2 receptor alpha	6.55	BCL3	B-Cell CLL/Lymphoma 3	-9.95
SOX9	Sex Determining Region Y)-Box 9	4.42	PTGER2	Prostaglandin E Receptor 2	-8.75
TNFRSF10B	Tumor Necrosis Factor Receptor Superfamily, Member 10b	3.16	IKKBK	inhibitor of nuclear factor kappa-B kinase	-8.73
SOD1	Superoxide dismutase	3.99	CRP	C-reactive protein	-8.35

EGR2	(Early Growth Response 2	3.86	PLAT	Plasminogen Activator	-7.41
CCR10	C-C chemokine receptor type 10	3.78	TLR2	Toll-like receptor 2	-6.09
VCAM1	Vascular cell adhesion protein 1	3.65	JAK2	Janus Kinase 2	-5.87
EDN1	Endothelin 1	3.63	MAP3K1	Mitogen-Activated Protein Kinase Kinase 1	-5.57
JUN	Jun Proto-Oncogene	3.54	ICAM1	Intercellular Adhesion Molecule 1	-5.55
PSMD3	26S proteasome non-ATPase regulatory subunit 3	3.38	C5	Complement Component 5	-4.78
NR4A1	Nuclear Receptor Subfamily 4	3.31	LTB4R2	Leukotriene B4 Receptor 2	-4.33
IGFBP2	Insulin-Like Growth Factor Binding Protein 2	2.91	NFKB1	Nuclear factor NF-kappa-B p105	-4.18
RARA	Retinoic acid receptor alpha	2.48	IGFBP1	Insulin-Like Growth Factor Binding Protein 1	-4.17
TGFB1	Transforming growth factor beta	2.46	PLCB4	Phospholipase C, Beta 4	-4.09
			CCL2	Chemokine (C-C Motif) Ligand 2	-3.99
			TRAF2	TNF receptor-associated factor 2	-3.98
			STAT3	Signal Transducer And Activator Of Transcription 3	-3.83
			CSF2	Colony Stimulating Factor 2 Receptor	-3.7
			TNFRSF1A	Tumor Necrosis Factor Receptor Superfamily, Member 1A	-3.54
			CREB1	CAMP Responsive Element Binding Protein 1	-3.32
			NFKB2	Nuclear Factor Of Kappa Light Polypeptide Gene Enhancer In B-Cells 2	-3.32
			IGFBP3	Insulin-Like Growth Factor Binding Protein 3	-3.16
			EGFR	Epidermal Growth Factor Receptor	-2.95
			REL	v-rel avian reticuloendotheliosis viral oncogene homolog	-2.84
			NFKB1	Nuclear factor NF-kappa-B p105 subunit	-2.78
			TGFBR1	Transforming Growth Factor, Beta Receptor 1	-2.77
			IL1RN	Interleukin 1 Receptor Antagonist	-2.74
			TP53	tumor protein p53	-2.43
			MALT1	Mucosa-associated lymphoid tissue lymphoma translocation protein 1	-2.35
			RELB	V-Rel Avian Reticuloendotheliosis Viral Oncogene Homolog B	-2.34
			MAPK8	Mitogen-Activated Protein Kinase 8	-2.09

Values are expressed as fold change in gene expression relative to vehicle treated control cells. Positive and negative values indicate up- and down-regulation of gene expression, respectively. A fold difference cut-off point was set at ≥ 2.5 .

Table 2: List of genes that were differentially dysregulated in cancerous ACHN cells compared to untreated RPTEC/TERT1 cells

Genes with increased expression			Genes with decreased expression		
Gene	Gene name	Fold increase	Gene	Gene name	Fold decrease
VCAM1	Vascular cell adhesion molecule 1	185.52	IL1R1	Interleukin (IL)1-receptor 1	-53.30
CCR10	Chemokine (C-C Motif) Receptor 10	23.24	HDLA	major histocompatibility complex, class I, A	-51.65
CTGF	Connective Tissue Growth Factor	20.88	IL1RN	interleukin (IL)1-receptor 1	-46.38
IGFBP2	Insulin-Like Growth Factor Binding Protein 2	18.96	SOD2	Superoxide dismutase 2	-41.10
RETN	Resistin	5.86	NR4A2	Nuclear receptor related 1 protein	-39.13
MMP2	Matrix Metalloproteinase 2	3.99	TRAF3	TNF receptor-associated factor 3	-29.53
ADRB2	Adrenoceptor Beta 2, Surface	3.53	TNFA	tumor necrosis factor a (TNF superfamily, member 2)	-27.81
STAT1	Signal Transducer And Activator Of Transcription 1	3.09	IL6	Interleukin 6	-24.24
PLCB4	Phospholipase C, Beta 4	3.08	IL6R	Interleukin 6 receptor	-21.16
EGR2	Early Growth Response-2	2.87	TRAF5	TNF receptor-associated factor 5	-20.59
PAI1	Plasminogen activator inhibitor-1	2.08	CRP	C-reactive protein	-18.65
IL2RA	(Interleukin 2 Receptor, Alpha	6.11	CXCL1	Chemokine (C-X-C Motif) Ligand 1	-17.67
TRAF1	TATA Box Binding Protein (TBP)-Associated Factor	3.58	ICAM1	Intercellular Adhesion Molecule 1	-16.81
TLR4	Toll-Like Receptor 4	2.55	JAK2	Janus Kinase 2	-16.79
			IGFBP3	Insulin-Like Growth Factor Binding Protein 3	-15.28
			CSF2	Colony Stimulating Factor 2 Receptor, Alpha	-14.84
			SOX9	Transcription factor SOX-9	-13.78
			IL23	Interleukin-23	-13.60
			MAP3K1	Mitogen-Activated Protein Kinase Kinase Kinase 1	-12.45
			CSF1	Colony Stimulating Factor 2 Receptor, Alpha	-10.66
			CXCL2	Chemokine (C-X-C Motif) Ligand 2	-9.45
			TGFBR1	Transforming Growth Factor, Beta Receptor 1	-8.77
			VEGFA	Vascular Endothelial Growth Factor A	-8.62
			PTGER2	Prostaglandin E Receptor 2 (Subtype EP2)	-8.50
			BCAM	Basal Cell Adhesion Molecule	-8.10

			CASP1	Caspase 1, Apoptosis-Related Cysteine Peptidase	-8.07
			BCL6	B-cell lymphoma 6 protein	-7.80
			IKBKB	liases for IKBKB Gene	-7.22
			TNFRSF10A	Tumor Necrosis Factor Receptor Superfamily, Member 10	-6.30
			SCOS3	Inhibitor Of Kappa Light Polypeptide Gene Enhancer In B-Cells	-6.07

Values are expressed as fold change in gene expression relative to vehicle treated control cells. Positive and negative values indicate up- and down-regulation of gene expression, respectively. A fold difference cut-off point was set at ≥ 2.5 .

Table 3: Summary of genes that were dysregulated in both carcinogen (KBrO₃) treated RPTEC/TERT1 and in cancerous ACHN cells compared to the untreated RPTEC/TERT1 cells

Upregulated	Downregulated
CTGF	BCL3
PAI1	CASP1
VCAM1	CCL2
RETN	CCL20
CCR10	CREB1
IGFBP2	CRP
ADRB2	CSF2
EGR2	CXCL1
PAI1	CXCL2
IL2RA	ICAM1
	IGFBP1
	IGFBP3
	IKBKB
	IL1R1
	IL1RN
	IL6
	IL8
	JAK2
	LTB4R2
	MAP3K1
	MYD88
	NFKB1
	NFKB1
	NFKB2
	PTGER2
	REL
	RELB
	STAT3
	TGFBR1
	TLR2

	TLR3
	TNFRSF1A
	TP53
	TRAF2
	TRAF3
	TRAF5
	TRAF6

3.4. Curcumin effectively reduced KBrO₃ induced TRAF3 and IL1-R1 downregulation and CTGF upregulation

To validate the results of the PCR array, individual TaqMan- based probe assays were used to measure the expression of TRAF3, IL1-R1, and CTGF quantitatively using qRT-PCR. The exposure of RPTEC/TERT1 to 5.5mM KBrO₃ significantly ($p < 0.001$) inhibited TRAF3 and IL-1R1 gene expression compared to untreated or curcumin-treated cells (*Fig.3a and 3b*). In contrast, KBrO₃ treatment significantly ($p < 0.01$) upregulated CTGF gene expression in KBrO₃-treated RPTEC/TERT1 compared with untreated or curcumin-treated cells (*Fig.3c*). More importantly, the co-treatment of 25 μ M curcumin with KBrO₃ significantly ($p < 0.05$) diminished the negative effect of KBrO₃ on TRAF3 expression (*Fig.3a*), and induced a significant ($p < 0.01$) reduction of the overexpressed CTGF level when combined with KBrO₃ compared with KBrO₃ alone (*Fig.3c*). However, the protective effect of curcumin on KBrO₃ induced IL-1R1 suppression wasn't significant ($p > 0.05$), (*Fig.3b*).

For further validation, we investigated the expression of CTGF at the protein level. In this case, we compared the CTGF repressor activity of curcumin with silymarin, a natural CTGF repressor[27] [28]. KBrO₃ clearly up-regulated CTGF protein expression, which was markedly repressed by curcumin. Strikingly, curcumin showed a higher CTGF repressor activity than silymarin when combined with KBrO₃ compared with KBrO₃-only treatment (*Fig. 3d*).

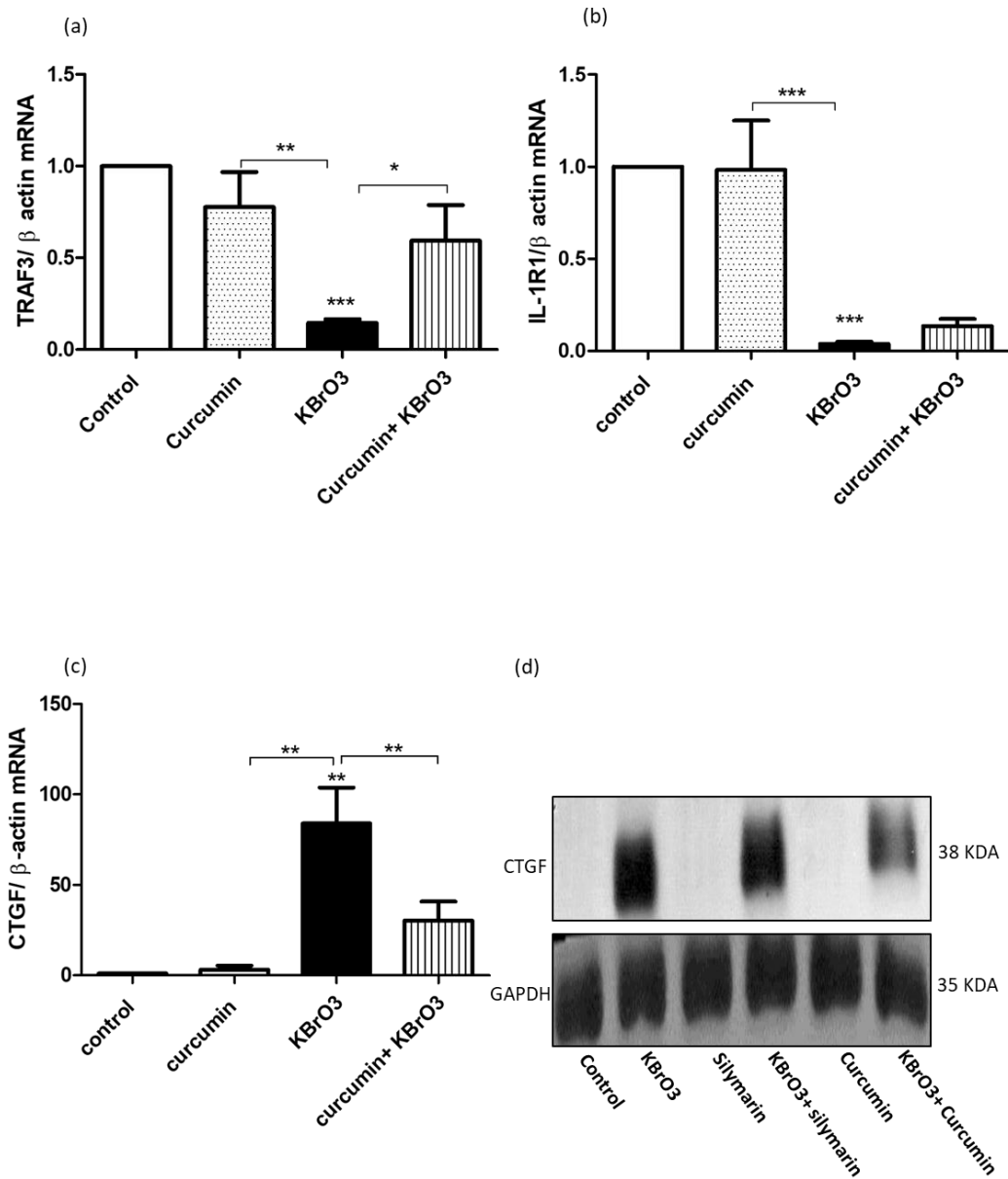


Figure 3. Analysis of the effects of KBrO₃ on TRAF3, IL-1R1, and CTGF gene expression, and the protective potential of curcumin.

Fig.3 a,b) KBrO₃ (5.5mM) treatment of RPTEC/TERT1 for 24h on TRAF3 and IL-1 gene expression, respectively compared with the untreated or curcumin-treated cells. The data represents three independent experiments. (*= $P > 0.05$)

Fig.3 c,d) KBrO₃ (5.5mM)- treatment of RPTEC/TERT1 for 24h on CTGF at both mRNA and protein levels in comparison the untreated or curcumin-treated cells. The data represents three independent experiments (**= $P < 0.01$)

3.5. Curcumin diminishes the deciliating effects of the genotoxic carcinogen KBrO₃

It has been reported that some renal carcinogens including KBrO₃ induce ciliary loss [23]. For this reason, we investigated whether curcumin has a protective potential against KBrO₃-induced deciliation. As shown in

Fig.4a (i) and (ii), RPTEC/TERT1 cells were treated with 0.1% DMSO (control) or with 25 μ M curcumin. Under both conditions, RPTEC/TERT1 exhibited well-defined tight junctional barriers between cells (green), and prominent cilia (red). Treating cells with 5.5mM KBrO₃ (iii) resulted in disruption of the tight junctional protein ZO-1 and a complete loss of the ciliary marker protein, acetylated α -tubulin. The co-treatment of curcumin with KBrO₃ (iv) minimized ciliary loss and junctional protein damage.

To confirm the results, we investigated the effect of KBrO₃ on Arl13b, a specific ciliary protein, using confocal microscopy. Very prominent and intact cilia were observed in both untreated and curcumin-treated cells, as shown in *Fig.4b (i) and (ii)*, respectively. The exposure of RPTEC/TERT1 cells to 5.5mM KBrO₃ for 24h caused a significant loss of cilia. In contrast, the co-treatment of 25 μ M curcumin with KBrO₃ clearly reduced the deciliating effect of KBrO₃ on RPTEC/TERT1 cells (*Fig.4b iv*).

We also examined gene expression levels of ZO-1 and Arl13b using TaqMan probe-based gene assays, *Fig.4c and 4d*. As seen in both figures, KBrO₃ at 5.5 mM significantly down-regulated the expression of both ZO-1 ($p<0.05$) and Arl13b ($p<0.01$) compared with untreated or curcumin-treated cells. However, the co-treatment of 25 μ M curcumin with KBrO₃ significantly ($p<0.01$) reversed the negative effect of KBrO₃ on ZO-1 and Arl13b gene expression.

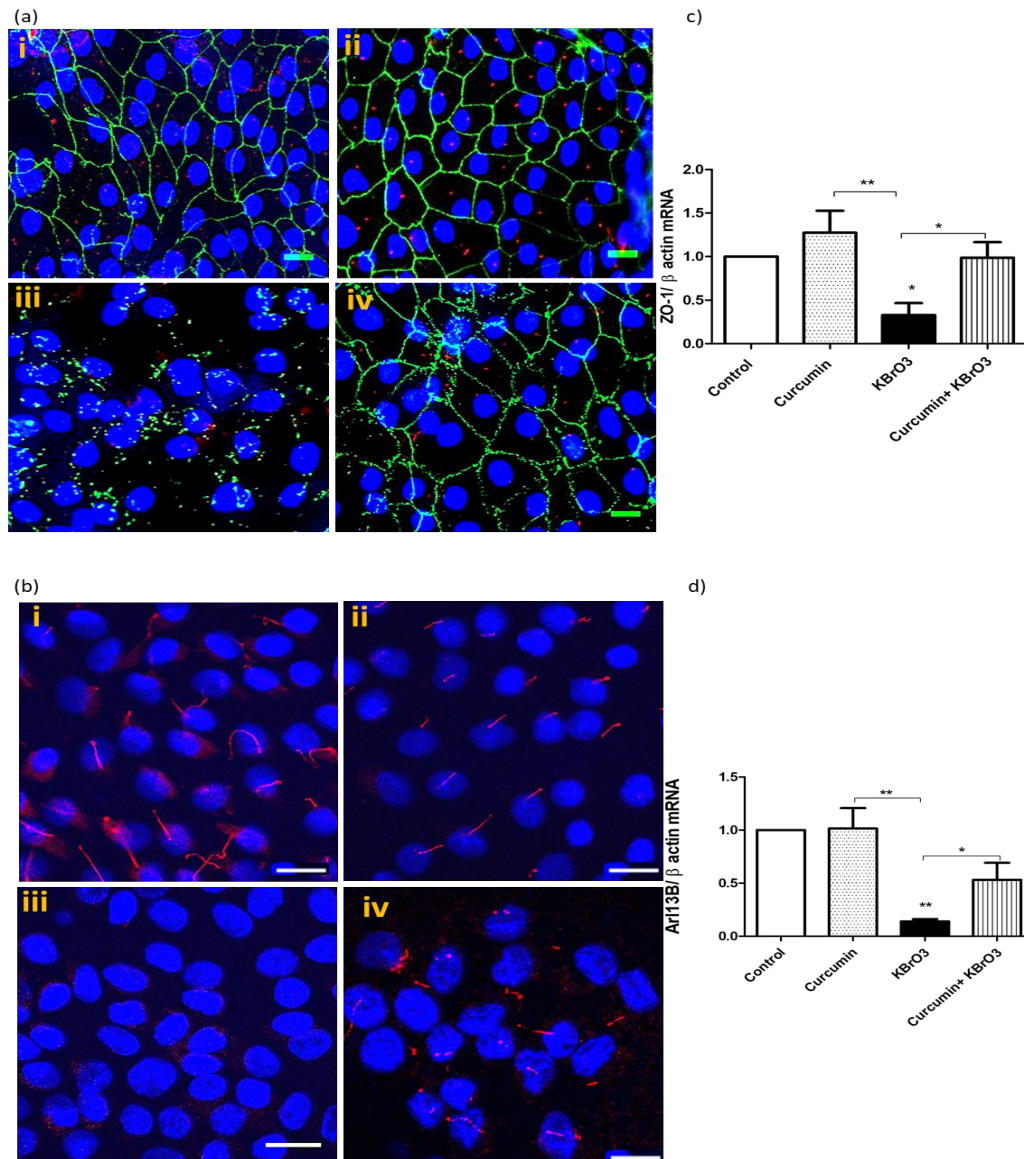


Figure 4. Effect of Curcumin on KBrO₃ induced loss of primary cilia and disruption of tight junction proteins

Fig.4a) KBrO₃ (5.5mM) treatment of RPTEC/TERT1 for 24h on ciliary and junctional proteins in comparison with untreated or curcumin-treated cells. RPTEC/TERT1 cells were cultured in 8-well chamber slides and treated with after 10 days of 100% confluency. Confocal images (40x) show the primary cilia with red labelled, α -acetylated tubulin, while the green staining represents the tight junctional protein ZO-1. Hoechst 33342 was used to stain the nuclei (blue), scale 50 μ m. (i) 0.1% DMSO (control), (ii) curcumin 25 μ M, (iii) 5.5 mM KBrO₃ (ic10), (iv) Co-treatment of curcumin + KBrO₃. The images are representative of 3 independent experiments. Scale =50 μ m.

Fig.4b KBrO₃ (5.5mM) treatment of RPTEC/TERT1 for 24h on a ciliary protein in comparison with untreated or curcumin-treated cells. Confocal images (40x) show the primary cilia with red labelled Arl13b. Hoechst 33342 was used to stain the nuclei (blue), scale 50 μ m. (i) 0.1% DMSO (control), (ii) curcumin 25 μ M, (iii) 5.5 mM KBrO₃ (ic10), (iv) Co-treatment of curcumin + KBrO₃. The images are representative of 3 independent experiments

Fig.4c,d) KBrO₃ (5.5mM) treatment of RPTEC/TERT1 for 24h on ZO-1 and Arl13b gene expression, respectively compared with the untreated or curcumin-treated cells. The data represents three independent experiments. * = $p > 0.05$, ** = $p > 0.01$.

4. Discussion

Potassium bromate, KBrO₃, a salt of the bromate ion, is a nephrotoxic and neurotoxic agent in humans and a proven carcinogen in animals [29, 30]. KBrO₃ is considered a possible human carcinogen (IIb) according to the International Agency for Research on Cancer (IARC) [31]. It was used as a model of cancers in many *in vivo* studies [4, 32-34].

The cytotoxic effects of KBrO₃ were previously assessed by measuring the activity of the lactate dehydrogenase (LDH) enzyme. Akanji *et al* found that after administration of a single dose of KBrO₃, LDH activity was significantly increased in rat renal and intestinal tissues compared to other tissues [35]. In addition, Ahmed *et al* reported that the release of LDH from KBrO₃-treated cells was linked to KBrO₃-induced oxidative stress [36]. In our model, we found that the co-treatment of KBrO₃ with curcumin resulted in decreased LDH release which reflects the protective potential of curcumin against KBrO₃-induced cytotoxicity. Curcumin has antioxidant, anti-inflammatory, and free radical scavenging activity. Its structure provides two methoxyphenyl groups and an enol form of β -diketone which illicit typical radical trapping activity [37].

In this study, treating human renal RPTEC/TERT1 cells with IC₁₀ or IC₅₀ concentrations of KBrO₃ caused an increase of H₂O₂ and 8-OHdG levels suggesting that the induction of oxidative stress is one of the mechanisms by which KBrO₃ induces its toxic and carcinogenic effects. We measured H₂O₂ levels as it is more stable than other oxidative species; also, H₂O₂ represents the precursor molecule of the hydroxyl radical that directly targets DNA and forms DNA adducts [38]. The co-treatment of KBrO₃ with curcumin suppressed KBrO₃ induced elevation of H₂O₂ and 8-OHdG levels at both toxic and subtoxic concentrations. Our findings are in line with a number of previous studies [39-42]. 8-OHdG is a biomarker for oxidative stress and carcinogenicity [43, 44] and has been proven to be a factor in initiating and promoting the process of carcinogenesis [45]. It has been reported that reactive species such as reactive oxygen species (ROS) can attack nucleotide pools such as dGTP forming 8-OHdG. The adduct formed can bind adenine and cytosine nucleotide

bases causing A:G mismatch. If the mismatch is irreparable, G:C to A:T transversion, a mutation will form. This mutation is mainly detected in many proto-oncogenes and tumor suppressor genes. In addition, the formation of DNA adducts such as 8-OHdG can cause steric hindrance which affect the fidelity of DNA replication [46]. 8-OHdG is considered as an important biomarker to measure the extent of DNA damage following the exposure to cancer initiating agents. Furthermore, it is also considered as a cofactor of cancer initiation and promotion [47]

Curcumin's chemopreventive potential has been proven by many *in vitro* and *in vivo* studies. Much research has shown that curcumin can efficiently protect cells from H₂O₂-induced oxidative cell injury [38, 48]. Due to its antioxidant potential, curcumin was shown to have the ability to reduce lipid peroxidation and DNA damage, while increasing the level of vitamin C, vitamin E, and total anti-oxidant capacity [49, 50]. Furthermore, curcumin has been shown to induce phase II metabolism while suppressing phase I metabolizing enzymes such as renal ornithine decarboxylase [51]. Because the catalase enzyme potentially detoxifies and decomposes H₂O₂ to H₂O [52], the activation of catalase by curcumin is considered another effective way to counteract oxidative stress. In this study, KBrO₃ was shown to suppress the anti-oxidant catalase enzyme which represents one mechanism by which KBrO₃ increases oxidative stress in cells. Our finding is in agreement with a previous study [53]. Interestingly, curcumin effectively reversed KBrO₃ induced catalase suppression, which suggests that this may be an important mechanism by which curcumin mediates its chemopreventive effects. Taken together, we can conclude that curcumin blocked the carcinogenic potential of KBrO₃ by increasing catalase enzyme activity thus reducing H₂O₂ and 8-OHdG levels.

Previous studies have shown that oxidative DNA damage causes activation of many inflammatory genes which creates a positive feedback loop leading to increased DNA damage, thus promoting cellular transformation and tumor progression [54-56]. Therefore to determine the role of inflammatory genes in our model, we measured a total of 192 target genes following the treatment of RPTEC/TERT1 cells with a subtoxic concentration of KBrO₃ and compared the dysregulation status of the genes with the congruent genes in a human renal cancerous ACHN cell line. We found that CTGF was the most overexpressed gene following KBrO₃ treatment and the third most overexpressed gene in the cancerous ACHN cell line. To our knowledge, this is the first study to provide evidence of the increased expression of CTGF following KBrO₃ treatment at both transcriptional and translational levels. There is abundant evidence from previous studies showing that CTGF can be overexpressed by oxidative stress conditions [57-60], and it has also been shown that CTGF is up-regulated in many cancers [61-64] including renal cell carcinomas [65]. Taken together, we propose that the carcinogenic potential of KBrO₃ might be through DNA adduct formation and the dysregulation of several inflammatory-regulating genes including CTGF. We also compared the potential CTGF repressor activity of curcumin with silymarin, another chemopreventive agent with a well-known CTGF repressor activity [27, 66-68]. Co-treatment of curcumin with KBrO₃ significantly reduced the expression of CTGF at both RNA and protein levels. Our results are consistent with Zheng and Chen who found that curcumin reduced CTGF overexpression by interfering with upstream TGF- β signaling and TGF- β receptor activation. In addition to this, curcumin was found to induce GSH antioxidant synthesis and peroxisome proliferator-activated receptor (PPAR)- γ activation. Furthermore, curcumin was shown to modulate extracellular matrix gene expression such as α 1(I)-collagen fibronectin and α -smooth muscle actin (α -SMA) by interrupting TGF- β signaling including

its downstream effector, CTGF [69]. Curcumin halted the CTGF pathway via inhibition of ERK, P38 MAPK, and NF- κ B pathways [70-72].

We have also shown that treating human renal RPTEC/TERT1 cells with KBrO₃ negatively affected ciliary and junctional protein expression. KBrO₃ caused a reduction in the number of ciliated cells and disturbed cellular borders. Our group has previously reported that KBrO₃ induced RPTEC/TERT1 ciliary loss was accompanied by an increased proportion of cells at G2/S phase, and thus caused activation of cell cycle progression and proliferation [23]. We have found that curcumin protected RPTEC/TERT1 cells against KBrO₃ induced deciliation. Another study showed that curcumin exerted an anti-proliferative effect via inhibition of cell cycle regulators of hepatic cells when they were exposed to diethylnitrosamine, a genotoxic carcinogen [73]. Blackmore *et al.* found that curcumin targeted colorectal cancer cells by arresting the G2/M phase of the cell cycle through disruption of microtubular orientation and assembly, as well as chromosomal condensation and congression [74]. Taken together, these studies show that KBrO₃'s deciliating effect caused loss of cellular differentiation and promoted cellular proliferation. Strikingly, such negative effects of KBrO₃ were found to be significantly minimized by co-treatment with curcumin in our system.

We have also shown that treating cells with a subtoxic concentration of KBrO₃ caused inhibition of IL-1 and TRAF3 gene expression. However the impact of KBrO₃ was reduced when treated in combination with curcumin. IL-1 and TRAF3 were selected for further analysis due to their direct link with apoptosis-mediated cell death [75, 76]. Furthermore, it has been found that IL-1 can regulate ciliary length. For instance, a study by Wann and Knight showed that ciliary length increased by approximately 50% following only 3 hours of exposure to IL-1. The mechanism of ciliary elongation is through a protein kinase A (PKA) dependent mechanism [77]. Therefore, by inhibiting IL-1 gene expression, KBrO₃ can counteract apoptosis and induce cellular dedifferentiation. TRAF3 is a cytoplasmic component with E3 ubiquitin ligase activity; following the binding to CD40, TRAF3 activates B-lymphocyte cells. It has been found that mice homozygous for a null allele of TRAF3 develop B-cell lymphoma. It also participates in the inhibition of NF- κ B signaling pathway, namely interacting with Act 1 in cancer cells. Cells with mutant TRAF3 become cancerous due to the activation of NF- κ B [78]. Generally, TRAF3 controls an alternative pathway of NF- κ B activation with no effects on the classical pathway. TRAF3 negatively regulates NF- κ B inducing kinase (NIK) levels, therefore the mutation of TRAF3 genes or activation of receptor-mediated proteasomal degradation is associated with the accumulation and auto-phosphorylation of NIK and activation of IKK α , which leads to the activation of NF- κ B [79]. TRAF3 is sequestered to the cell cytoskeleton via TRAF3 interacting protein 1 (TRAF3ip1) which is localized to the cilium and is necessary for ciliogenesis. TRAF3ip1 mutant cells have been shown to be incapable of generating a primary cilium [80].

We have shown that KBrO₃ induced downregulation of NF- κ B gene expression at the mRNA level. However, no rescue effect was observed of curcumin against KBrO₃-induced NF- κ B downregulation (supplementary, Figure 1).

A study by Wann *et al* suggested that primary cilia are considered an important influence on NF- κ B activation, thus loss of cilia was associated with deregulation of NF- κ B activation [81]. Furthermore, Sinha *et al* found that TRAF3 can participate in NF- κ B activation through the x-linked ectodermal dysplasia receptor [82]. Therefore downregulation of TRAF3, NF- κ B, and IL-1 gene expression and disruption of cilia by KBrO₃ might be important mechanisms by which to counteract apoptosis and induce cellular dedifferentiation in

carcinogenesis. However, further studies are required to investigate the effect of ciliary loss on the expression of inflammatory genes.

A significant number of publications have described curcumin's anti-inflammatory potential as an important property to curtail the progression of several diseases including cancers. Curcumin shows potent anti-inflammatory potential due to its direct regulatory effects on several transcription factors such as STAT, MAPK, and NF-KB, interleukins (ILs) such as TNF- α , IL-1,2,6,8 and 12. Furthermore, it has shown to inhibit lipoxygenase, cyclooxygenase-2 (COX-2), and inducible nitric oxide synthase (iNOS) enzymes activities [83-85]

Despite the broad spectrum of curcumin's health benefits and the wide range of biological significance, its clinical applications are potentially limited due to poor bioavailability. The slight aqueous solubility, instability, and photo degradation of curcumin represent major obstacles that limit its use in different therapeutic applications. Therefore, more than 1500 papers had been published by 2015 to find suitable solutions for such fundamental dilemmas in the clinical use of curcumin [86]. Perhaps, the incorporation of curcumin in a phospholipid system to form a liposomal-curcumin complex is one of the successful trials to improve curcumin's bioavailability. Conjugation of liposomal curcumin with different molecules such as polyethylene glycol and folic acid has been reported to highly extend the biological half-life and targetability of the liposomal curcumin. Therefore, a substantial improvement of both pharmacokinetics and pharmacodynamics of curcumin molecules was recorded following the administration of liposomal curcumin *in vivo* [87]. Other strategies include induction of structural modifications to improve curcumin's *in vivo* stability and effectiveness. For instance, a recent study has shown that dimethoxy curcumin has a unique anti-tumor activity due to its ability to suppress the transcription factor activator protein-1 (AP-1) and induce degradation of androgen receptors (AR). At the same time, dimethoxy curcumin showed a high metabolic stability compared to curcumin itself [88]. While another study found that a modification in curcumin's aromatic ring resulted in the formation of 10 different curcumin analogues with more potent *in vitro* and *in vivo* anti-tumor activities than curcumin [89] In this study we provide significant evidence that the food additive KBrO₃ induced carcinogenic alteration via induction of ROS and activation of several oncogenic genes, counteracting tumor suppressor genes and favouring cell dedifferentiation. To our knowledge, this is the first study to identify the dysregulated genes of KBrO₃-treated normal kidney cells that might be implicated in KBrO₃-induced carcinogenesis via compare them with the genes of renal cancerous cells. Furthermore, this is the first study to report another protective mechanism of curcumin via inhibition of KBrO₃-induced cell dedifferentiation.

In conclusion, the molecular mechanisms of curcumin chemoprevention have been investigated and are due in particular to its potential to block KBrO₃ induced intracellular oxidative stress, DNA damage, and the dysregulation of signaling hubs that control inflammation, apoptosis, and cell differentiation which contribute to the pathogenesis and progression of KBrO₃-induced renal cancer. Although challenges such as poor absorption and rapid elimination represent the major roadblocks in curcumin's clinical applications, research is still ongoing to tackle these problems. However, the future seems bright particularly with the development of new curcumin analogues that are more potent, with higher bioavailability. Therefore, curcumin has considerable scope as a novel cancer prevention agent, due to its pleiotropic actions and in particular its cyto-protective and chemopreventive potential against chemical carcinogenesis.

Conflict of interests:

The authors declare no conflict of interests

Acknowledgement:

We are grateful to **the** Iraqi government (MHESR) for fully funding this study, and providing the financial support to undertake all experiments, **and to Science Foundation Ireland for funding the UCD Centre for Toxicology, where this project was undertaken**

References

1. Radford, R., et al., *Mechanisms of Chemical Carcinogenesis in the Kidneys*. International Journal of Molecular Sciences, 2013. **14**(10): p. 19416-19433.
2. FDA, *Potassium bromate*. 2016: USA, <http://www.accessdata.fda.gov/scripts/cdrh/cfdocs/cfcfr/CFRSearch.cfm?fr=172.730>.
3. Ishidate, M. and K. Yoshikawa, *Chromosome Aberration Tests with Chinese Hamster Cells in vitro with and without Metabolic Activation — A Comparative Study on Mutagens and Carcinogens*, in *Further Studies in the Assessment of Toxic Actions: Proceedings of the European Society of Toxicology Meeting, Held in Dresden, June 11 – 13, 1979*, P.L. Chambers and W. Klinger, Editors. 1980, Springer Berlin Heidelberg: Berlin, Heidelberg. p. 41-44.
4. Kasai, H., et al., *Oral administration of the renal carcinogen, potassium bromate, specifically produces 8-hydroxydeoxyguanosine in rat target organ DNA*. Carcinogenesis, 1987. **8**(12): p. 1959-1961.

5. DeAngelo, A.B., et al., *Carcinogenicity of potassium bromate administered in the drinking water to male B6C3F1 mice and F344/N rats*. Toxicol Pathol, 1998. **26**(5): p. 587-94.
6. Shiao, Y.H., et al., *Mutations in the VHL gene from potassium bromate-induced rat clear cell renal tumors*. Cancer Lett, 2002. **187**(1-2): p. 207-14.
7. Ballmaier, D. and B. Epe, *Oxidative DNA damage induced by potassium bromate under cell-free conditions and in mammalian cells*. Carcinogenesis, 1995. **16**(2): p. 335-342.
8. Parsons, J.L. and J.K. Chipman, *The role of glutathione in DNA damage by potassium bromate in vitro*. Mutagenesis, 2000. **15**(4): p. 311-316.
9. Ballmaier, D. and B. Epe, *DNA damage by bromate: Mechanism and consequences*. Toxicology, 2006. **221**(2-3): p. 166-171.
10. Bader, H.L. and T. Hsu, *Systemic VHL gene functions and the VHL disease*. Febs Letters, 2012. **586**(11): p. 1562-1569.
11. Michaud, E.J. and B.K. Yoder, *The Primary Cilium in Cell Signaling and Cancer*. Cancer Research, 2006. **66**(13): p. 6463-6467.
12. Pan, J., T. Seeger-Nukpezah, and E.A. Golemis, *The role of the cilium in normal and abnormal cell cycles: emphasis on renal cystic pathologies*. Cellular and Molecular Life Sciences, 2013. **70**(11): p. 1849-1874.
13. Quarumby, L.M. and J.D.K. Parker, *Cilia and the cell cycle?* The Journal of Cell Biology, 2005. **169**(5): p. 707-710.
14. Schraml, P., et al., *Sporadic clear cell renal cell carcinoma but not the papillary type is characterized by severely reduced frequency of primary cilia*. Mod Pathol, 2009. **22**(1): p. 31-6.
15. Mehta, R.G., et al., *Cancer chemoprevention by natural products: how far have we come?* Pharm Res, 2010. **27**(6): p. 950-61.
16. Aggarwal, B.B., et al., *Curcumin: the Indian solid gold, in The molecular targets and therapeutic uses of curcumin in health and disease*. 2007, Springer. p. 1-75.
17. Steward, W.P. and K. Brown, *Cancer chemoprevention: a rapidly evolving field*. British Journal of Cancer, 2013. **109**(1): p. 1-7.
18. Chendil, D., et al., *Curcumin confers radiosensitizing effect in prostate cancer cell line PC-3*. Oncogene, 2004. **23**(8): p. 1599-1607.
19. Gupta, S.C., et al., *Discovery of curcumin, a component of golden spice, and its miraculous biological activities*. Clinical and Experimental Pharmacology and Physiology, 2012. **39**(3): p. 283-299.
20. Uzzan, B. and R. Benamouzig, *Is Curcumin a Chemopreventive Agent for Colorectal Cancer?* Current Colorectal Cancer Reports, 2016. **12**(1): p. 35-41.

21. Momtazi, A.A., et al., *Curcumin as a MicroRNA Regulator in Cancer: A Review*. Rev Physiol Biochem Pharmacol, 2016. **171**: p. 1-38.
22. Banikazemi, Z., et al., *Diet and cancer prevention: Dietary compounds, dietary MicroRNAs, and dietary exosomes*. Journal of Cellular Biochemistry, 2018. **119**(1): p. 185-196.
23. Radford, R., et al., *Carcinogens induce loss of the primary cilium in human renal proximal tubular epithelial cells independently of effects on the cell cycle*. Am J Physiol Renal Physiol, 2012. **302**(8): p. F905-16.
24. Wieser, M., et al., *hTERT alone immortalizes epithelial cells of renal proximal tubules without changing their functional characteristics*. Am J Physiol Renal Physiol, 2008. **295**(5): p. F1365-75.
25. Robertson, R., et al., *The Anti-Inflammatory Effect of Algae-Derived Lipid Extracts on Lipopolysaccharide (LPS)-Stimulated Human THP-1 Macrophages*. Marine Drugs, 2015. **13**(8): p. 5402.
26. Buchmann, K., L. Pedersen, and J. Glamann, *Humoral immune response of European eel *Anguilla anguilla* to a major antigen in *Anguillicola crassus* (Nematoda)*. Diseases of Aquatic Organisms, 1991. **12**(1): p. 55-57.
27. Tzeng, J.I., et al., *Silymarin decreases connective tissue growth factor to improve liver fibrosis in rats treated with carbon tetrachloride*. Phytotherapy Research, 2013. **27**(7): p. 1023-1028.
28. Duval, F., et al., *Protective mechanisms of medicinal plants targeting hepatic stellate cell activation and extracellular matrix deposition in liver fibrosis*. Chinese Medicine, 2014. **9**: p. 27.
29. IARC, *IARC MONOGRAPHS ON THE EVALUATION OF THE CARCINOGENIC RISK OF CHEMICALS TO HUMANS; Some Naturally Occurring and Synthetic Food Components, Furocoumarins and Ultraviolet Radiation*. 1986: Volume 40, Lyon -France, P 207-220. p. 207-220.
30. Geter, D.R., et al., *Kidney Toxicogenomics of Chronic Potassium Bromate Exposure in F344 Male Rats*. Translational Oncogenomics, 2006. **1**: p. 33-52.
31. IARC, *Evaluation of carcinogenic risks to humans. Overall Evaluations of Carcinogenicity: An Updating of IARC Monographs*. 1987, : Supplement 7, volume 1-42, Lyon, France, page 70 p. 70.
32. Kurokawa, Y., et al., *Long-term in vivo carcinogenicity tests of potassium bromate, sodium hypochlorite, and sodium chlorite conducted in Japan*. Environmental Health Perspectives, 1986. **69**: p. 221-235.
33. Kurokawa, Y., et al., *Dose-Response Studies on the Carcinogenicity of Potassium Bromate in F344 Rats After Long-Term Oral Administration*. Journal of the National Cancer Institute, 1986. **77**(4): p. 977-982.
34. Sakamoto, K., et al., *MUTYH-Null Mice Are Susceptible to Spontaneous and Oxidative Stress-Induced Intestinal Tumorigenesis*. Cancer research, 2007. **67**(14): p. 6599-6604.
35. Akanji, M., M. Nafiu, and M. Yakubu, *Enzyme activities and histopathology of selected tissues in rats treated with potassium bromate*. African Journal of Biomedical Research, 2008. **11**(1).
36. Ahmad, M.K., et al., *Chemoprotective effect of taurine on potassium bromate-induced DNA damage, DNA-protein cross-linking and oxidative stress in rat intestine*. PLoS One, 2015. **10**(3): p. e0119137.

37. Masuda, T., et al., *Chemical Studies on Antioxidant Mechanism of Curcumin: Analysis of Oxidative Coupling Products from Curcumin and Linoleate*. Journal of Agricultural and Food Chemistry, 2001. **49**(5): p. 2539-2547.
38. Mahakunakorn, P., et al., *Cytoprotective and cytotoxic effects of curcumin: dual action on H₂O₂-induced oxidative cell damage in NG108-15 cells*. Biol Pharm Bull, 2003. **26**(5): p. 725-8.
39. Kurokawa, Y., et al., *Toxicity and carcinogenicity of potassium bromate--a new renal carcinogen*. Environmental Health Perspectives, 1990. **87**: p. 309-335.
40. Giri, U., M. Iqbal, and M. Athar, *Potassium bromate (KBrO₃) induces renal proliferative response and damage by elaborating oxidative stress*. Cancer Lett, 1999. **135**(2): p. 181-8.
41. Khan, R.A., et al., *Potassium bromate (KBrO₃) induced nephrotoxicity: protective effects of n-hexane extract of Sonchus asper*. Journal of Medicinal Plants Research, 2011. **5**(25): p. 6017-6023.
42. Khan, R.A., M.R. Khan, and S. Sahreen, *Protective effects of rutin against potassium bromate induced nephrotoxicity in rats*. BMC complementary and alternative medicine, 2012. **12**(1): p. 204.
43. Kasai, H., *Analysis of a form of oxidative DNA damage, 8-hydroxy-2'-deoxyguanosine, as a marker of cellular oxidative stress during carcinogenesis*. Mutat Res, 1997. **387**(3): p. 147-63.
44. Nakae, D., T. Umemura, and Y. Kurokawa, *Reactive oxygen and nitrogen oxide species-induced stress, a major intrinsic factor involved in carcinogenic processes and a possible target for cancer prevention*. Asian Pac J Cancer Prev, 2002. **3**: p. 313-318.
45. Valavanidis, A., T. Vlachogianni, and C. Fiotakis, *8-hydroxy-2' -deoxyguanosine (8-OHdG): A Critical Biomarker of Oxidative Stress and Carcinogenesis*. Journal of Environmental Science and Health, Part C, 2009. **27**(2): p. 120-139.
46. Klaunig, J.E., L.M. Kamendulis, and B.A. Hocevar, *Oxidative stress and oxidative damage in carcinogenesis*. Toxicol Pathol, 2010. **38**(1): p. 96-109.
47. Valavanidis, A., C. Vlachogianni T Fau - Fiotakis, and C. Fiotakis, *8-hydroxy-2' -deoxyguanosine (8-OHdG): A critical biomarker of oxidative stress and carcinogenesis*. 2009(1532-4095 (Electronic)).
48. Cohly, H.H.P., et al., *Effect of Turmeric, Turmerin and Curcumin on H₂O₂-Induced Renal Epithelial (LLC-PK1) Cell Injury*. Free Radical Biology and Medicine, 1998. **24**(1): p. 49-54.
49. Rai, B., et al., *Possible action mechanism for curcumin in pre-cancerous lesions based on serum and salivary markers of oxidative stress*. J Oral Sci, 2010. **52**(2): p. 251-6.
50. Ciftci, G., et al., *Therapeutic role of curcumin in oxidative DNA damage caused by formaldehyde*. Microsc Res Tech, 2015. **78**(5): p. 391-5.

51. Iqbal, M., Y. Okazaki, and S. Okada, *Curcumin attenuates oxidative damage in animals treated with a renal carcinogen, ferric nitrilotriacetate (Fe-NTA): implications for cancer prevention*. *Molecular and Cellular Biochemistry*, 2009. **324**(1): p. 157-164.
52. Petrucci, R.H., *General Chemistry: Principles & Modern Applications (9th ed.)*. 2007: Prentice Hall.
53. Watanabe, S., et al., *Potassium bromate-induced hyperuricemia stimulates acute kidney damage and oxidative stress*. *Journal of health science*, 2004. **50**(6): p. 647-653.
54. Coussens, L.M. and Z. Werb, *Inflammation and cancer*. *Nature*, 2002. **420**(6917): p. 860-867.
55. Reuter, S., et al., *Oxidative stress, inflammation, and cancer: How are they linked?* *Free radical biology & medicine*, 2010. **49**(11): p. 1603-1616.
56. Halliday, G.M., *Inflammation, gene mutation and photoimmunosuppression in response to UVR-induced oxidative damage contributes to photocarcinogenesis*. *Mutation Research/Fundamental and Molecular Mechanisms of Mutagenesis*, 2005. **571**(1-2): p. 107-120.
57. Ohshiro, Y., et al., *Reduction of diabetes-induced oxidative stress, fibrotic cytokine expression, and renal dysfunction in protein kinase C β -null mice*. *Diabetes*, 2006. **55**(11): p. 3112-3120.
58. Park, S.K., et al., *Hydrogen peroxide is a novel inducer of connective tissue growth factor*. *Biochem Biophys Res Commun*, 2001. **284**(4): p. 966-71.
59. Branchetti, E., et al., *Oxidative stress modulates vascular smooth muscle cell phenotype via CTGF in thoracic aortic aneurysm*. *Cardiovascular Research*, 2013. **100**(2): p. 316-324.
60. Matsuda, S., et al., *Induction of connective tissue growth factor in retinal pigment epithelium cells by oxidative stress*. *Jpn J Ophthalmol*, 2006. **50**(3): p. 229-34.
61. Wenger, C., et al., *Expression and differential regulation of connective tissue growth factor in pancreatic cancer cells*. *Oncogene*, 1999. **18**(4): p. 1073-1080.
62. Jiang, W.G., et al., *Differential expression of the CCN family members Cyr61, CTGF and Nov in human breast cancer*. *Endocrine-Related Cancer*, 2004. **11**(4): p. 781-791.
63. Chen, P.-P., et al., *Expression of Cyr61, CTGF, and WISP-1 correlates with clinical features of lung cancer*. *PloS one*, 2007. **2**(6): p. e534.
64. Chu, C.-Y., et al., *Connective tissue growth factor (CTGF) and cancer progression*. *Journal of biomedical science*, 2008. **15**(6): p. 675-685.
65. Chintalapudi, M.R., et al., *Cyr61/CCN1 and CTGF/CCN2 mediate the proangiogenic activity of VHL-mutant renal carcinoma cells*. *Carcinogenesis*, 2008. **29**(4): p. 696-703.
66. ZHAO, Y.-z., et al., *Effect of silymarin on expression of TGF- β 1 and CTGF of hepatic fibrosis in rats [J]*. *China Journal of Modern Medicine*, 2010. **15**: p. 010.

67. LIU, Z.-g., et al., *Research Progress in Pharmacological Effects of Silymarin [J]*. Journal of Liaoning University of Traditional Chinese Medicine, 2012. **10**: p. 036.
68. Yang, C.H., et al., *SHSST- cyclodextrin complex inhibits TGF- β /Smad3/CTGF to a greater extent than silymarin in a rat model of carbon tetrachloride- induced liver injury*. Molecular Medicine Reports, 2015. **12**(4): p. 6053-6059.
69. Zheng, S. and A. Chen, *Curcumin suppresses the expression of extracellular matrix genes in activated hepatic stellate cells by inhibiting gene expression of connective tissue growth factor*. American Journal of Physiology - Gastrointestinal and Liver Physiology, 2006. **290**(5): p. G883-G893.
70. O'Connell, M. and S. Rushworth, *Curcumin: potential for hepatic fibrosis therapy?* British journal of pharmacology, 2008. **153**(3): p. 403-405.
71. Chen, A. and S. Zheng, *Curcumin inhibits connective tissue growth factor gene expression in activated hepatic stellate cells in vitro by blocking NF- κ B and ERK signalling*. British Journal of Pharmacology, 2008. **153**(3): p. 557-567.
72. Deng, Y.-T., et al., *Arecoline-stimulated connective tissue growth factor production in human buccal mucosal fibroblasts: Modulation by curcumin*. Oral Oncology, 2009. **45**(9): p. e99-e105.
73. Chuang, S.-E., et al., *Inhibition by curcumin of diethylnitrosamine-induced hepatic hyperplasia, inflammation, cellular gene products and cell-cycle-related proteins in rats*. Food and Chemical Toxicology, 2000. **38**(11): p. 991-995.
74. Blakemore, L.M., et al., *Curcumin-induced mitotic arrest is characterized by spindle abnormalities, defects in chromosomal congression and DNA damage*. Carcinogenesis, 2012.
75. Georgopoulos, N.T., et al., *A novel mechanism of CD40-induced apoptosis of carcinoma cells involving TRAF3 and JNK/AP-1 activation*. Cell Death Differ, 2006. **13**(10): p. 1789-801.
76. England, H., et al., *Release of interleukin-1alpha or interleukin-1beta depends on mechanism of cell death*. J Biol Chem, 2014. **289**(23): p. 15942-50.
77. Wann, A.K. and M.M. Knight, *Primary cilia elongation in response to interleukin-1 mediates the inflammatory response*. Cell Mol Life Sci, 2012. **69**(17): p. 2967-77.
78. Edwards, S.K., et al., *N-benzyladriamycin-14-valerate (AD 198) exhibits potent anti-tumor activity on TRAF3-deficient mouse B lymphoma and human multiple myeloma*. BMC cancer, 2013. **13**(1): p. 481.
79. Hacker, H., P.H. Tseng, and M. Karin, *Expanding TRAF function: TRAF3 as a tri-faced immune regulator*. Nat Rev Immunol, 2011. **11**(7): p. 457-68.
80. Berbari, N.F., et al., *Mutations in Traf3ip1 reveal defects in ciliogenesis, embryonic development, and altered cell size regulation*. Dev Biol, 2011. **360**(1): p. 66-76.

81. Wann, A.K., J.P. Chapple, and M.M. Knight, *The primary cilium influences interleukin-1beta-induced NFkappaB signalling by regulating IKK activity*. Cell Signal, 2014. **26**(8): p. 1735-42.
82. Sinha, S.K., et al., *Role of TRAF3 and -6 in the activation of the NF-kappa B and JNK pathways by X-linked ectodermal dysplasia receptor*. J Biol Chem, 2002. **277**(47): p. 44953-61.
83. Deguchi, A., *Curcumin targets in inflammation and cancer*. Endocr Metab Immune Disord Drug Targets, 2015. **15**(2): p. 88-96.
84. Karimian, M.S., et al., *Curcumin as a natural regulator of monocyte chemoattractant protein-1*. Cytokine & Growth Factor Reviews, 2017. **33**(Supplement C): p. 55-63.
85. Shehzad, A., et al., *Multifunctional Curcumin Mediate Multitherapeutic Effects*. Journal of Food Science, 2017. **82**(9): p. 2006-2015.
86. Kasi, P.D., et al., *Molecular targets of curcumin for cancer therapy: an updated review*. Tumor Biology, 2016. **37**(10): p. 13017-13028.
87. Feng, T., et al., *Liposomal curcumin and its application in cancer*. International Journal of Nanomedicine, 2017. **12**: p. 6027-6044.
88. Teymouri, M., et al., *Biological and pharmacological evaluation of dimethoxycurcumin: A metabolically stable curcumin analogue with a promising therapeutic potential*. Journal of Cellular Physiology, 2018. **233**(1): p. 124-140.
89. Zhang, L., et al., *Discovery of novel anti-tumor curcumin analogues from the optimization of curcumin scaffold*. Medicinal Chemistry Research, 2017. **26**(10): p. 2468-2476.